DOI: 10.13009/EUCASS2017-430

CFD Study of Vorticity Patterns and Sound Generation in Simplified Aft–Finocyl Geometries

M. Laureti[⋆†]*, G. Rossi*[⋆]*, B. Favini*[⋆] *and R. Paciorri*[⋆]
[⋆]*Dept. of Mechanical and Aerospace Engineering - Sapienza University of Rome*
Via Eudossiana 18, Rome, Italy 00184
mariasole.laureti@uniroma1.it · giacomo.rossi@uniroma1.it · bernardo.favini@uniroma1.it · renato.paciorri@uniroma1.it
E. Cavallini[⋆⋆]
[∗]*Italian Space Agency ASI - Scientific Research Division*
Via del Politecnico snc - 00133, Rome, Italy
enrico.cavallini@asi.it
A. Neri[⋆⋆⋆]
[⋆⋆⋆]*ESA ESRIN - VEGA Integrated Project Team*
Via Galileo Galilei 00044 Frascati (Rome), Italy
agostino.neri@esa.int
[†]*Corresponding author*

Abstract

The generation of vorticity patterns, in simplified aft-finocyl geometries of interest, is investigated by means of 2D-axisymmetric ILES CFD simulations with a 2^{nd} order TVD scheme. The development of vortical shear layer structures is observed along the propellant surface and across the finocyl region. These structures are found to induce sustained pressure oscillations as due to the coupling of vorticity and acoustic modes of the chamber. The qualitative and quantitative characterization of the pressure oscillations phenomenon, in terms of both amplitude and frequencies, is a challenging problem, indeed it results to be strongly affected by mesh level, order of accuracy an sub-grid model of ILES approach.

1. Introduction

During the operative life of many solid rocket motors (SRMs), sustained low-level pressure oscillations may occur.[1–6] Although they do not compromise the SRM integrity, performances are dramatically reduced. Furthermore they result in thrust oscillations which have to be taken in account in the assessment of induced dynamic environment involving the entire launch vehicle system, in order to guarantee the safety and comfort of the payload. The evolution of the flowfield in the combustion chamber during the firing may lead to the development of complex vorticity patterns, especially for aft-finocyl SRMs, that may give rise to pressure oscillations as result of the coupling whit acoustic modes of the chamber. Since pressure oscillations are originated in the combustion chamber,[7–9] a careful analysis of the flow field is necessary to explain their origin. It is worth noting that not all aft-finocyl SRMs exhibit pressure oscillations as it may be evinced by experimental evidences and numerical simulations. As concerns P80, first stage of VEGA launcher, SFTs performed during the launcher development phase and flights show the presence of sustained pressure oscillations at the first longitudinal mode of the combustion chamber.[7,8,10–12] A similar scenario appears for POD-Y,[13,14] the mid scale demonstrator for pressure oscillations of the possible future evolutions of P80. The comparison between P80 and POD-Y shows that pressure oscillations amplitude scales roughly proportional with the motor scale (P80 SRM is more than three times bigger than the POD-Y SRM), whereas Z23 and Z9, respectively 2^{nd} and 3^{rd} stage of VEGA, are not prone to classical pressure oscillations scenario. Full 3D-ILES CFD simulations on Z23 exhibit a very low level pressure oscillations which results in both axial and lateral thrust fluctuations of the order 1% of the overall thrust delivered by the SRM.[8] The amplitude of pressure unsteady component is at maximum 50 mbar, this level is also the minimum value observed in the class of aft-finocyl grains with metallized propellant. On the basis of experimental and numerical collected data, both the motor scale and the propellant grain geometry are expected to play a role on pressure oscillations onset and level. Numerical simulations performed up to now,[15–17] show that quantitative characterization of the phenomenon, in terms of amplitude and spectra, is a challenging problem because it results particularly delicate from numerical modelling stand point. Indeed numerical method, order of accuracy and

Copyright © 2017 by M. Laureti, G. Rossi, B. Favini, R. Paciorri, E. Cavallini and A. Neri. Published by the EUCASS association with permission.

DOI: 10.13009/EUCASS2017-430

grid resolution affect the aeroacoustic feedback-loop. CFD simulations on ZEFIRO 23[8] show also that the sub-grid model, in certain configuration, can bring about a drain of energy of the flowfield towards its high frequency modes resulting into an aeroacoustic coupling that involves very organized limit-cycle oscillations.

The aim of this paper is the investigation of the role of geometry in vorticity patterns production into simplified aft-finocyl geometries and the possible coupling with the acoustic modes of the chamber. At the same time the attention is focused on numerical modelling, pressure oscillations features are thus characterized by means of an uncertainty/sensitivity analysis. Numerical simulations are assumed to be inviscid, unsteady and 2D-axisymmetric; viscous effects and turbulence are accounted by ILES (inviscid LES) approach. Several sub-grid models are developed and tested in the frame of 2^{nd} order TVD schemes, in order to see how small modifications on dissipative effects, introduced by the slope limiter, affect the possible onset of feedback loop mechanism. Grid convergence analysis is necessary to assess phenomenon mesh sensitivity, which results to be crucial in the pressure oscillations characterization. The introduction of a simplified non uniform combustion model allows to assess thermal effects on pressure oscillations features. The test case is a simplified geometry of an aft-finocyl booster or first stage. The flowfield analysis is carried out over a SRM geometrical configuration which is related to an early phase of the firing when head-end pressure assumes its maximum value and the aft-part/finocyl region is at around the maximum burning propellant surface condition. In the early phase of the firing, axisymmetric model provides a roughly approximation of the SRM geometry because of the presence of the 3D aft-finocyl region. Four different geometries are taken in account, namely FIRST, ZERO-A, ZERO-B and ZERO-C. FIRST has a constant port radius along the longitudinal axis. Head-end pressure matches the value obtained considering a burning surface of an aft-finocyl booster, or first stage, where the aft-finocyl region is inhibited. The simplicity of FIRST geometry allows an intimate study of the slope limiter calibration and thermal non uniformity effects on acoustic excitation levels and modes. Aft-finocyl region as well as the connection with the cylindrical part, are modelled in ZERO geometries, which are designed in order to carry out investigations on the role of the geometry on pressure oscillations features. Geometry is fixed during the simulation, in this way there is no need for re-meshing the computation domain in order to follow the evolution of the propellant grain during the SRM operative life. This approach allows to characterize SRM limit cycle condition, even if there are no informations on how the grain regression, and therefore the time evolution of the internal flowfield, affects aeroacoustic coupling.

2. Mathematical and Numerical Model

The investigation is performed by using unsteady 2D-Axisymmetric Euler set of governing equations for a single specie single-phase flow, where viscous terms and turbulence phenomena are account directly in the intrinsic characteristics of numerical scheme, as classical in the ILES approach. This choice is due to high turbulence resolution difficulties which arise for Reynolds numbers of the order of $10^5 - 10^7$, as those involved in such case of study. Compressible effects cannot be neglected since, while in the combustion chamber the flowfield is characterized by very low-Mach numbers, the flowfield immediately in front of the nozzle and in the nozzle itself is subjected to strong expansion and the Mach ranges from low subsonic to moderate supersonic conditions. The Euler system of conservation laws is solved by the method of lines. According to this technique: space and time discretization of a partial differential equation (PDE) are decoupled and separately analysed. The space discretization replaces space derivatives with algebraic approximations, thus an initial-boundary problem results in a initial value problem which can be solved with a time integrator. The accuracy of the method can be increased by the use of highly efficient reliable initial value ODE solvers which are able to achieve high accuracy orders avoiding extremely small time steps. In this work CFD simulations are performed by an in-house code based on finite volume approach on multi-block structured grids. A second order total variation diminishing (TVD) scheme is used for the spatial integration, whereas the time evolution is made by a third order explicit Runge-Kutta scheme.

2.1 Non-Uniform Combustion Model

Mass flow rate and energy of the combustion products, injected in the chamber, are not uniform because of the inhomogeneous propellant grain composition and therefore this phenomenon affects the vorticity production at the grain surface. In the numerical simulations a simplified non uniform combustion model is assumed. Mass and energy fluxes per unit area, at the boundary condition on the grain surface, are modified of a percentage value keeping unchanged the integral on the total surface. Although fluxes are not uniform in space, they are kept constant over time, that means the model is not closed, thus combustion and acoustics are not coupled. The introduction of a non uniform combustion model is expected to decrease the amplitude of pressure oscillations. Hot spots on the propellant surface radiate spheric acoustic waves which may stabilize the shear layer. Another effect of the grain inhomogeneity is the introduction of dispersed solid burning particles, typically alumina or uncombusted aluminium, within the gas phase. They release a

DOI: 10.13009/EUCASS2017-430

significant amount of heat affecting the fluctuating nature of the flowfield. Distributed combustion of aluminium is not considered in the present simplified model.

2.2 Slope Limiter

In the framework of TVD methods, the slope limiter is an essential aspect for non-linear stability which is related in turn to the amount of artificial dissipation introduced in the numerical solution. Five different slope limiter have been employed: Min-Mod[18] is the most dissipative whereas the Super-Bee[18] is the least dissipative one. Van-Leer[19] slope limiter is placed in the middle of the TVD zone and is characterized by a continuous function of r, that is the ratio between the slope at the previous cell and the slope at the actual cell. MC[20] slope limiter is designed to follow as long as possible the straight line which minimize the dispersion error. The mentioned slope limiters are well known in literature, whereas the new limiter MS is proposed by the authors.

$$\phi_{Super\,Bee}(r) = max\left[0, min\left(2r, 1\right), min\left(r, 2\right)\right]; \quad \lim_{r\to\infty} \phi_{Super\,Bee} = 2 \tag{1}$$

$$\phi_{MC}(r) = max\left[0, min\left(2r, \frac{1+r}{2}, 2\right)\right]; \quad \lim_{r\to\infty} \phi_{MC} = 2 \tag{2}$$

$$\phi_{Mod\,MC}(r) = max\left[0, min\left(2r, \frac{1+2r}{3}, \frac{4+r}{5}, 1.2\right)\right]; \quad \lim_{r\to\infty} \phi_{Mod\,MC} = 1.2 \tag{3}$$

$$\phi_{Van\,Leer}(r) = \frac{r+|r|}{1+|r|}; \quad \lim_{r\to\infty} \phi_{Van\,Leer} = 2 \tag{4}$$

$$\phi_{Min\,Mod}(r) = max\left[0, min\left(1, r\right)\right]; \quad \lim_{r\to\infty} \phi_{Min\,Mod} = 1 \tag{5}$$

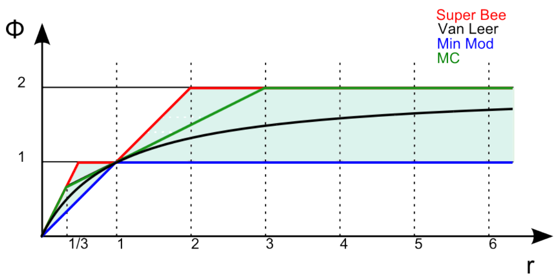

(a) Super Bee, Min Mod, Van Leer, MC Slope Limiters

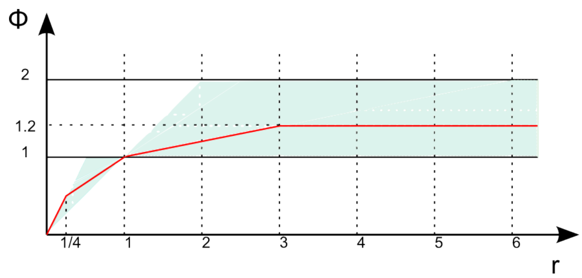

(b) MS slope limiter

Figure 1: Slope Limiters used for the Numerical Simulations

3. Simulations Set-Up

This study considers, as test case, a simplified geometry of a possible aft-finocyl booster or first stage, with some reference to a time instant and geometrical configuration which are known experimentally to be prone to pressure oscillations phenomena. The analysed geometries are presented in Fig.2. FIRST is the simplest one, whit a constant port radius along the longitudinal axis. Aft-finocyl region is modelled by additional volume in ZERO geometries. Furthermore a connection region, between the cylinder and the aft-finocyl part, is present in ZERO-A and ZERO-B. In the former case connection is sharp, in the latter cylinder and aft-finocyl region are joined together by a linear connection. On the grain surface, the boundary conditions are imposed in order to match the pressure in the test case combustion chamber during the selected phase of the firing. ZERO geometries are designed in order to qualitatively and quantitatively investigate the role of the SRM geometry in the generation of vorticity patterns, coupled with the fundamental acoustic modes of the combustion chamber, for the class of aft-finocyl SRM, starting from simplified cases of study. Also for these geometrical configurations non uniform combustion effects are investigated.

DOI: 10.13009/EUCASS2017-430

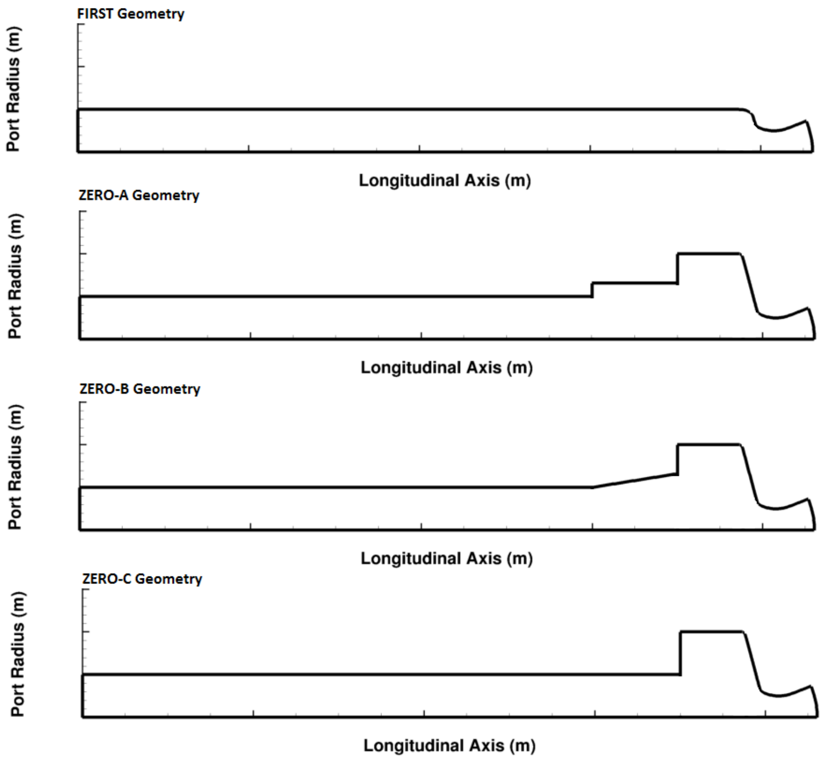

Figure 2: Semplified aft-finocyl Geometries of Interest

AS concerns the mesh, a multi-block structured grid is used. Mesh sensitivity and grid convergence analysis have been performed by computing solution on 2 grid levels. In order to reach a statistically steady solution, simulations have been computed on the coarse grid level first and carried on for a time long enough for solution to stabilize; then the solution has been interpolated on the finer grid and computed up to a statistically steady evolution. The coarse grid is obtained from the the finer by removing every other vertex along each coordinate line. The dimensions of the diadic grids, in terms of number of cells, are given in the Table 1.

Table 1: Number of Mesh-Grid Cells

	Coarse	**Fine**
FIRST	$\approx 11\,k$	$\approx 44\,k$
ZERO-A/B/C	$\approx 11\,k$	$\approx 44\,k$

Mass, momentum and energy fluxes per unit area of the propellant surface are kept constant during the simulation. Grain propellant combustion products are assumed to be perfect gases. It is worth noting the superior boundary of the cavity is treated as grain surface since, in this phase of the firing, the aft-end is almost completely filled by propellant. Symmetry boundary condition is imposed on the motor axis. Before chocking condition occurs, a subsonic outflow, with constant external pressure, is set at the nozzle exit. Once the flow in the divergent part is supersonic, the interface variables are extrapolated from the inside.

4. Results and discussion

4.1 FIRST

During the numerical simulations campaign, several slope limiters have been tested in the frame of 2^{th} order TVD schemes. Super-Bee and Min-Mod slope limiters enclose the TVD zone, the former represents the superior limit and the latter the inferior one. Non-linear stability characteristics of the selected numerical method are crucial for the success of simulations, Super-Bee slope limiter fails calculating flowfield solution. Whilst the robustness and reliability of the numerical method are connected to non-linear stability, dissipative effects may dump the smallest

DOI: 10.13009/EUCASS2017-430

scale structures destroying the onset of aeroacoustic coupling and limit cycles mechanisms. Using a Min-Mod slope limiter the flowfield reaches the steady state and there is not evidence of pressure oscillations. Among these two extreme cases, according to the slope limiter adopted in numerical simulations, several possible pressure oscillations scenarios appear.

Van Leer Slope Limiter

The flowfield computed by Van Leer slope limiter exhibits very low level, but present, pressure oscillations involving high frequencies near to the first transversal mode of the chamber. In the pressure oscillations spectra, two peaks, with comparable amplitude at slightly different frequencies, result in a beat phenomenon, where the envelope of the maxima and minima form a wave whose frequency is half the difference between the frequencies of the two original waves. Slope limiter affects the way vorticity field is resolved modifying its frequency, that is also modulated by the grid resolution. This observation is justified by the results obtained refining the mesh. Doubling the number of cells along the coordinate directions, the amplitude of pressure oscillations slightly rises up and the high frequencies disappear. The range of excited frequencies moves to lower values approaching the first longitudinal mode of the chamber, beat phenomenon is no longer present.

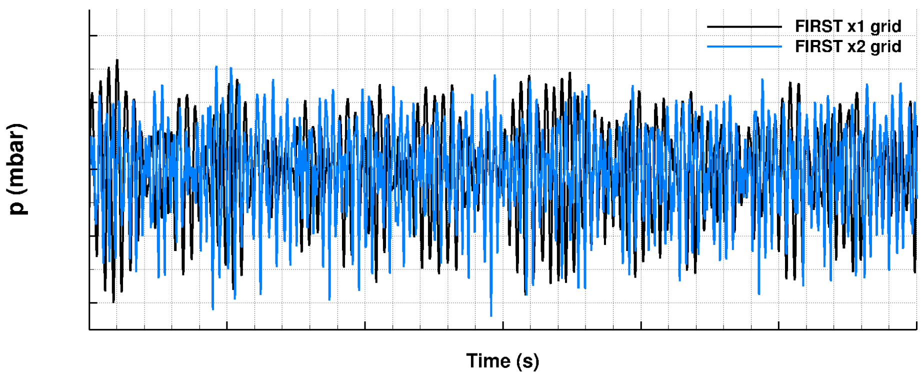

Figure 3: MS Slope Limiter: Resolution Effect on Unsteady Pressure over Time

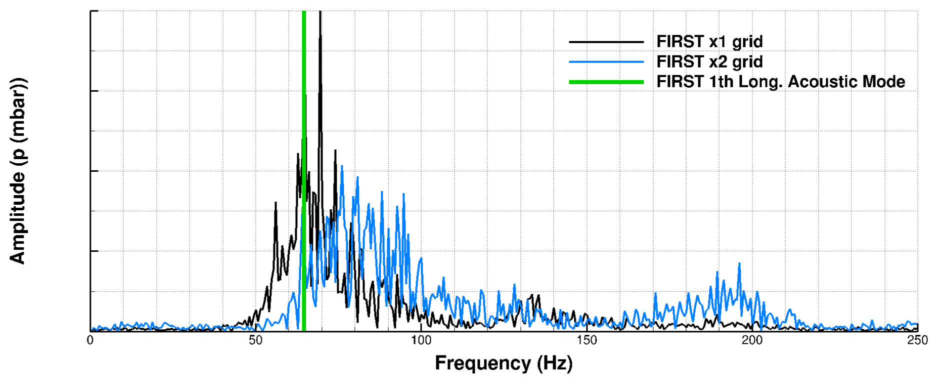

Figure 4: MS Slope Limiter: Resolution Effect on Unsteady Pressure Spectra

MC Slope Limiter

As concerns the solution obtained by means of MC slope limiter vorticity field and acoustic one are in feedback loop, bringing about the generation of sustained pressure. Once the limit cycle condition is reached, the amplitude of pressure oscillations is about one order of magnitude greater then the level computed by Van Leer slope limiter. The range of most excited frequency in the spectra is centred around the the first longitudinal acoustic mode of the chamber. Furthermore negligible frequency content is provided by the second longitudinal mode. Pressure oscillation

DOI: 10.13009/EUCASS2017-430

characteristics do not undergo to remarkable changes by refining the mesh grid. The amplitude keeps unchanged whereas the range of most excited frequencies enlarges and shifts slightly forward to higher values.

MS Slope Limiter

In order to understand how the slope limiter affects the solution in terms of pressure oscillations amplitude and spectra, MC slope limiter is gradually modified. Results show a remarkable level of uncertainty in the quantification of pressure oscillations characteristics. The slope of the limiter and its limit value act as calibration parameters. The TVD left zone, enclosed by the $\phi = 2r$, $\phi = r$ and $\phi = 1$, turns out to be crucial in the modulation of pressure oscillations amplitude, whereas the right zone affects moderately the oscillating field features. The more the slope limiter in the left zone approaches $\phi = r$, the more pressure oscillations amplitude reduces itself up to become null when the two straight lines coincide. MS slope limiter is designed to be placed about in the middle of the left zone, just like Van Leer, while its limit value is lower then the mean of MC and Min-Mod limit values. As well as the previous solution, the coupling between vorticity field and travelling pressure waves causes the onset of sustained pressure oscillations involving the first longitudinal chamber mode. Time evolution and spectra of pressure unsteady component for the coarse grid and the finest one are compared respectively in Fig.3 and Fig.4. The amplitude of pressure oscillations is about half the amplitude obtained by using MC slope limiter. In the spectra two peaks, near the first longitudinal mode, may be observed. Changing the mesh grid resolution the amplitude of the pressure unsteady component remains the same. Maximum peaks in pressure oscillations spectra have lower amplitudes because the signal energy is distributed on a larger range of excited frequencies. Indeed it results shifted towards high values, as seen in Fig.4.

It is worth noting that unsteady pressure component 2D-map has a plane wave structure: since pressure value is approximately uniform on the SRM radius, the field may be considered mono-dimensional. Although unsteady velocity components are related to unsteady pressure, their field is characterized by 2D-structure because of the presence of recirculation areas, as shown by instantaneous streamlines in Fig.6. Non-linear stability properties make MS limiter suitable for the study of pressure oscillations phenomenon, for this reason it is set for all the following numerical simulations.

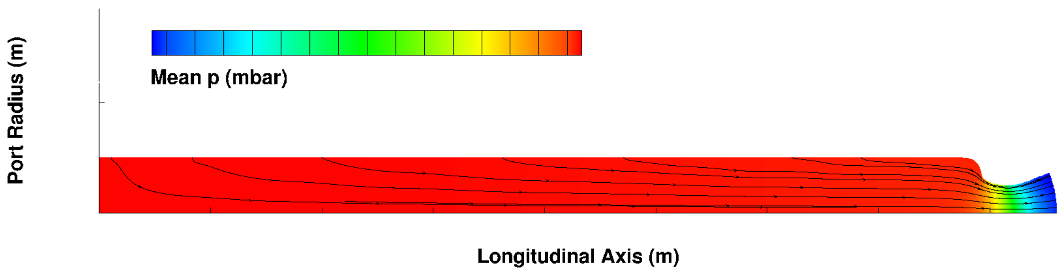

Figure 5: MS Slope Limiter:2D-Map of Mean Pressure Field

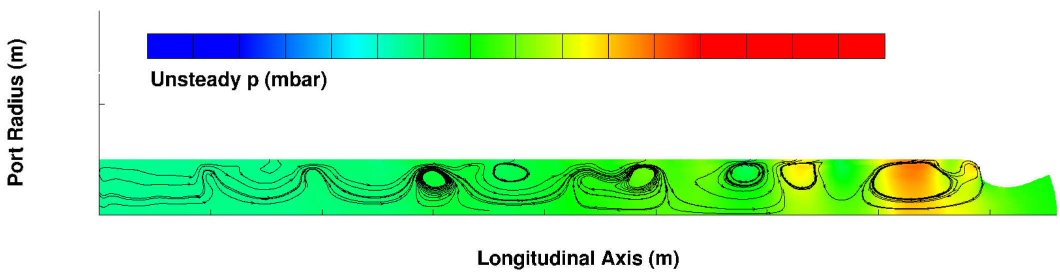

Figure 6: MS Slope Limiter:2D-Map of Unsteady Pressure Field

Pressure oscillations amplitude obtained in FIRST geometry is too much high if compared to the level exhibited by aft-finocyl SRM which are known to be not prone to classical pressure oscillations scenario. The introduction of a non uniform combustion model is expected to decrease the amplitude of pressure oscillations because of the stabilizing effect on the shear layer by acoustic waves generated by hot spots placed on the propellant grain surface. The results obtained with a non uniformity percentage value varying between 5% and 20% are compared to the solution

DOI: 10.13009/EUCASS2017-430

computed by the uniform combustion model. Percentage values higher then 10% are not inherent to real conditions nevertheless this assumption allows to assess the effect of non uniform combustion on the internal flowfield and pressure oscillations quantitative characterization. Fig.7 shows the higher is the non uniformity the more pressure oscillations amplitude decreases. Amplitude reduces of 20%, 85% and 92% moving from 0% non uniformity value to 5%, 10% and 20% respectively. The introduction of non uniform combustion model moves the vorticity frequency away from first longitudinal acoustic mode, inducing a gradual decoupling of vorticity field and acoustics, as can be seen in Fig.8. The lack of resonance effect makes pressure oscillations amplitude to decrease. Augmenting the non uniformity level, the range of excited frequencies enlarges that means combustion becomes noisier. Pressure oscillations amplitude, obtained whit 10% of non-uniformity, is taken as reference value for the simulations on ZERO geometries.

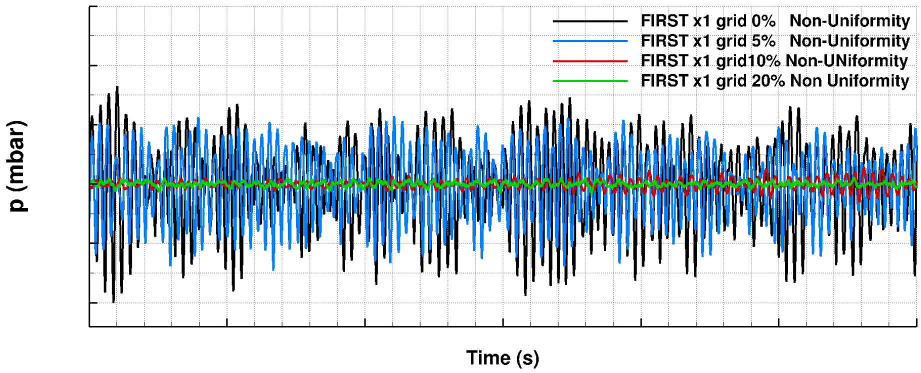

Figure 7: Non Uniform Combustion Effect on Unsteady Pressure over Time

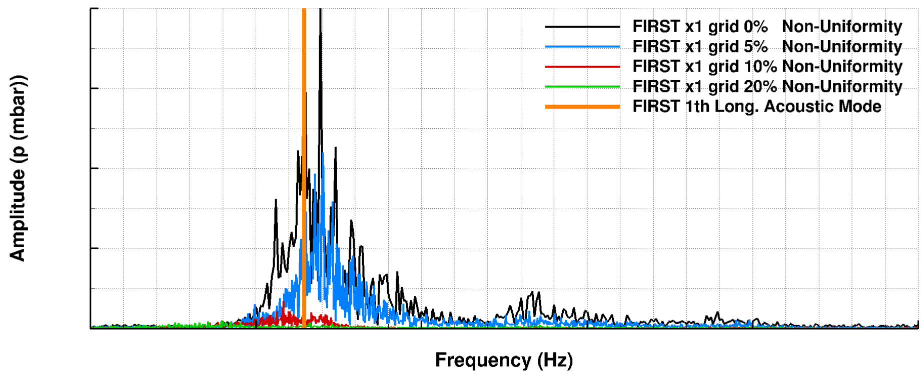

Figure 8: Non Uniform Combustion Resolution Effect on Unsteady Pressure Spectra

4.2 ZERO-A

Simplified geometries of a possible booster or first stage are considered. ZERO-A geometry is characterised by a steep connection region between cylinder and aft-finocyl region. In the selected configuration head-end pressure matches the value of the reference test case in a early phase of the firing. Since in this phase the aft-finocyl burning surface represents over 60% (including the star-shaped connection region) of the total surface, pressure is much higher than in FIRST, where the grain consists of a cylinder only and therefore respective flowfields are different. The frequency associated to the first longitudinal acoustic mode decreases with the respect to first longitudinal acoustic mode of FIRST SRM due to the introduction of aft-finocyl region and connection zone. The spectra of pressure oscillation, obtained by changing mesh resolution, is represented in Fig.10. Two separated peaks may be observed in the coarse level spectra: the lower frequency is related to vorticity field, whereas the second is connected to pressure waves; feedback-loop is thus absent. The convergence analysis stresses the mesh sensitivity effects on pressure oscillations phenomenon. Moving from the coarse mesh level to the finer, amplitude increases of 50%, as evinced by looking at Fig.9. The range

DOI: 10.13009/EUCASS2017-430

of excited frequencies in the spectra undergoes to dramatically modification: there are no longer two separated peaks, indeed vorticity frequency approaches the first longitudinal acoustic mode enhancing the coupling between the fields.

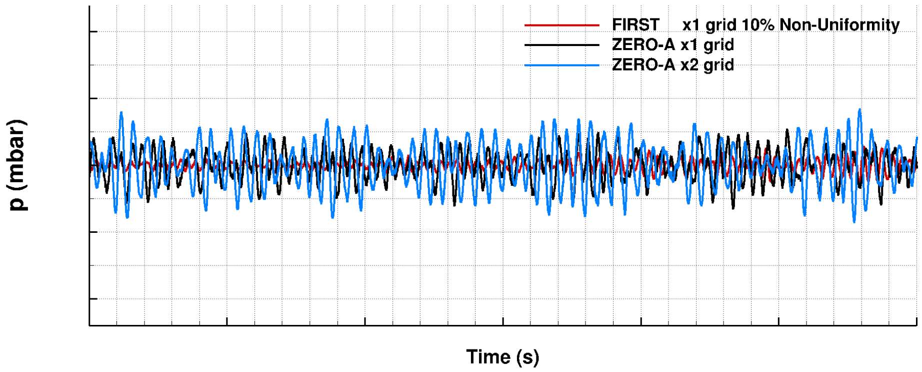

Figure 9: Resolution Effect on Unsteady Pressure over Time

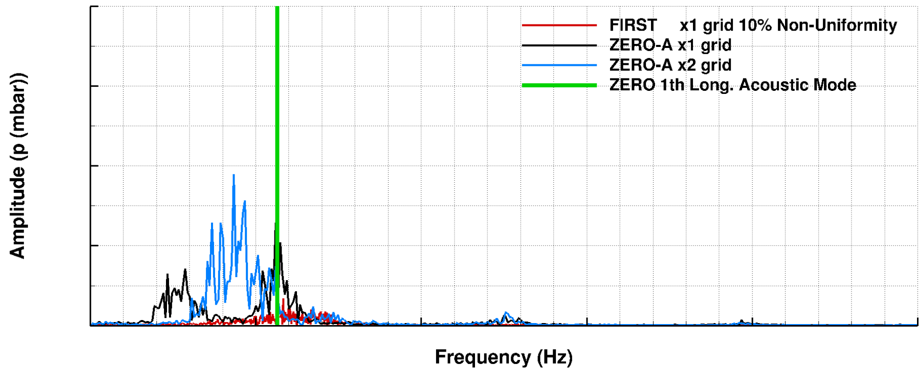

Figure 10: Resolution Effect on Unsteady Pressure Spectra

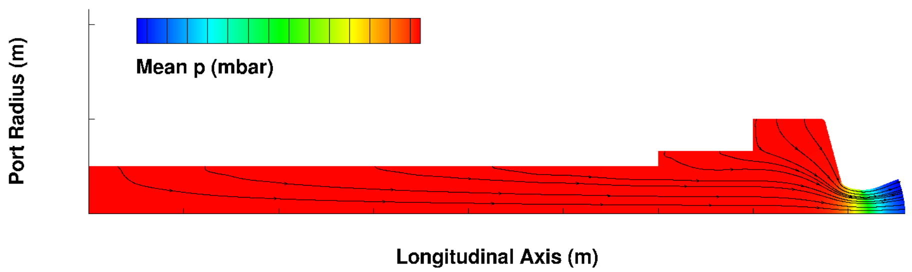

Figure 11: 2D-Map of Mean Pressure Field

DOI: 10.13009/EUCASS2017-430

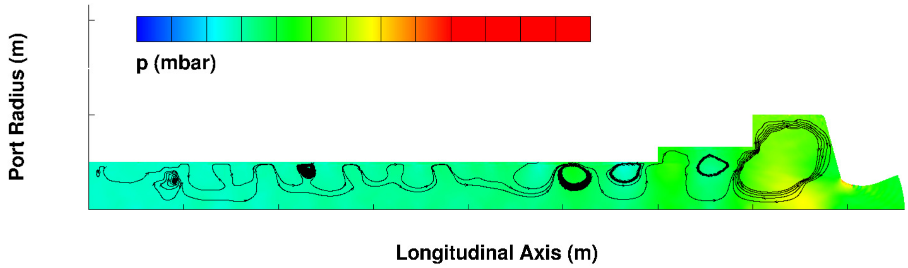

Figure 12: 2D-Map of Unsteady Pressure Field

Results obtained for ZERO-A configuration allows to observe the effect of geometry on pressure oscillations features as due to the shear layer detachment at grain propellant geometrical discontinuity around the connection region. The 2D-map of pressure unsteady component, represented in Fig.12, shows a plane wave structure in the cylindrical part, as in FIRST SRM, whereas the presence of the connection region and the aft-finocyl cavity alter the field introducing 2D effects. The 2D structure of unsteady velocity components field is connected to the characteristic dynamic of recirculation regions, as can be seen in FIRST SRM. The thermal effects due to the introduction of a non uniform combustion model are now discussed. Looking at Fig.13 it may be noted that the presence of high non uniformity percentage level does not modify the amplitude of pressure oscillations. The effect of the shear layer detachment at connection region discontinuity prevails on thermal effect.

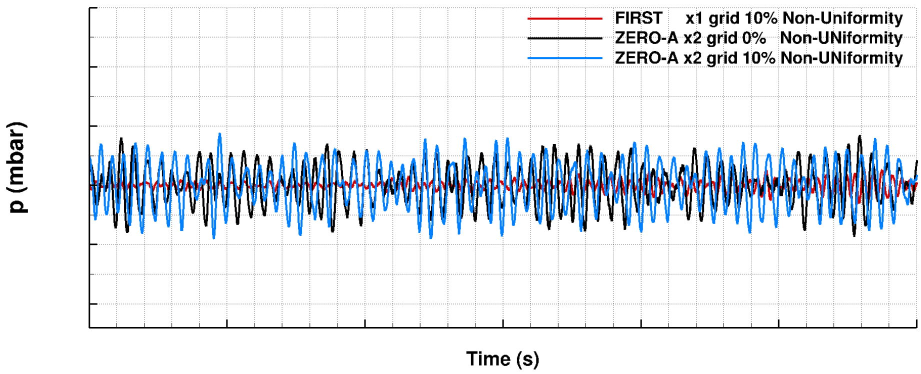

Figure 13: Non Uniform Combustion Effect on Unsteady Pressure over Time

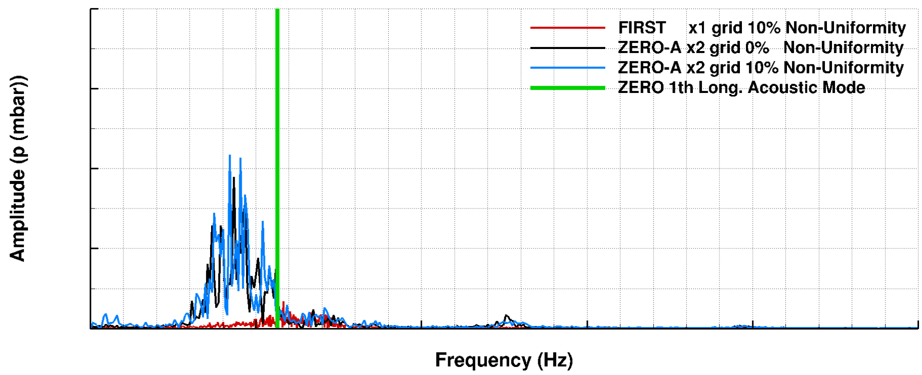

Figure 14: Non Uniform Combustion Effect on Unsteady Pressure Spectra

DOI: 10.13009/EUCASS2017-430

4.3 ZERO-B and ZERO-C

The internal flowfield and pressure oscillations features are expected to be modify by changing the shape of the connection region between cylinder and aft-finocyl part. In ZERO-B geometry these two grain sections are joined together by means of a linear connection. ZERO-C geometry is characterised by the absence of the connection region, thus aft-finocyl region is directly bounded to the cylinder. As concerns mesh sensitivity analysis, similar considerations can be made for ZERO-B and ZERO-C geometries. Coarse grid does not allow to resolve flowfield small structures, the vorticity frequency is much lower then the first acoustic longitudinal mode of the chamber so vorticity field and acoustic one cannot be coupled. ZERO-B spectra, presented in Fig.16, shows two separated ranges of excited frequencies with comparable energy content, ZERO-C spectra in instead more broad-band like. Refining the mesh, the vorticity field is better resolved, in particular the corner effect around the connection region. The frequency of vortices moves close to the frequency of pressure waves, producing a partial feedback-loop mechanism which results in a moderate pressure oscillations amplitude increase. This observation is particularly true for ZERO-C geometry: looking at fine mesh pressure oscillation spectra (Fig.18), it may be noted that vorticity frequency almost overlaps the a longitudinal acoustic mode of the chamber. Being the coupling enhanced for ZERO-C geometry, amplitude variation rate, obtained by comparing mesh levels, is higher then the one computed in ZERO-B geometry, as seen in Fig.17.

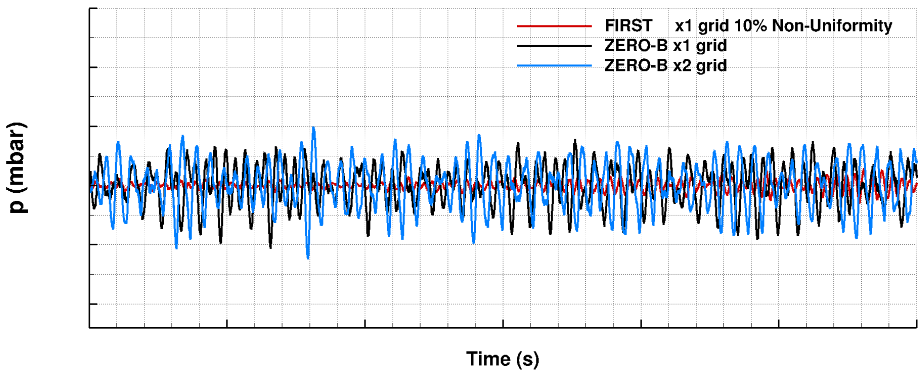

Figure 15: Resolution Effect on Unsteady Pressure over Time

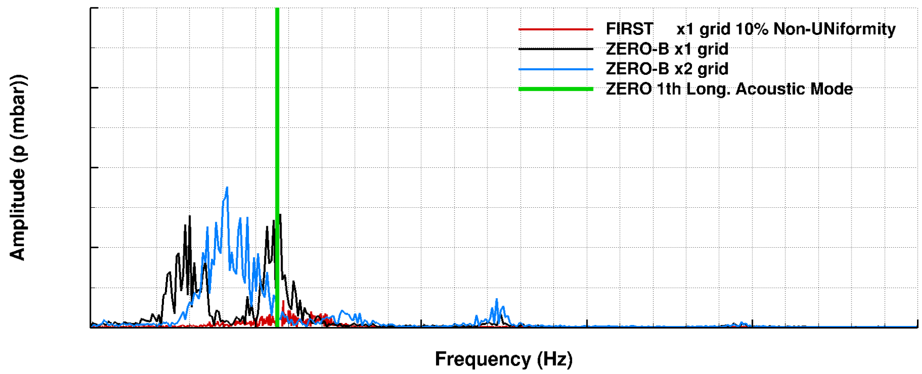

Figure 16: Resolution Effect on Unsteady Pressure Spectra

DOI: 10.13009/EUCASS2017-430

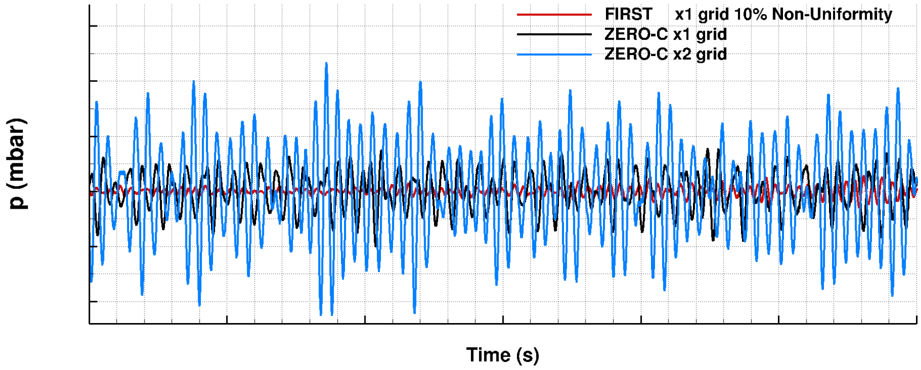

Figure 17: Resolution Effect on Unsteady Pressure over Time

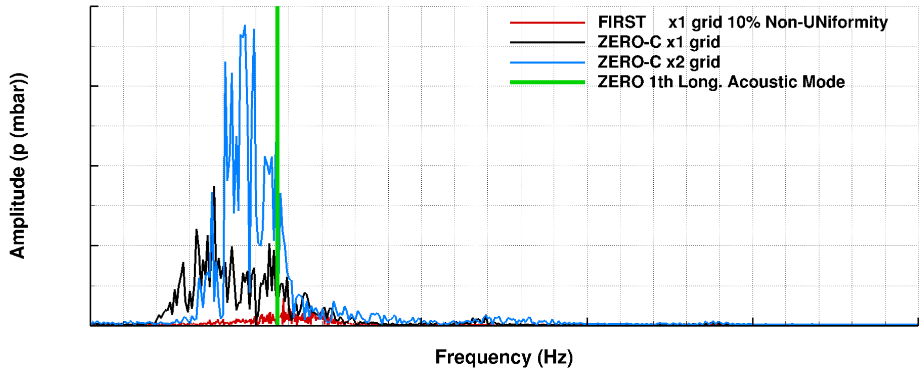

Figure 18: Resolution Effect on Pressure Spectra

As observed for ZERO-A geometry, pressure oscillations level is not substantially altered by the introduction of non-uniform combustion model. Although in the spectra peaks associated to non-uniform mass and energy fluxes are higher, the energy content of unsteady component of pressure is comparable in both cases, but it is distributed in a different way over the frequencies, as can be seen in Fig.20 and 22.

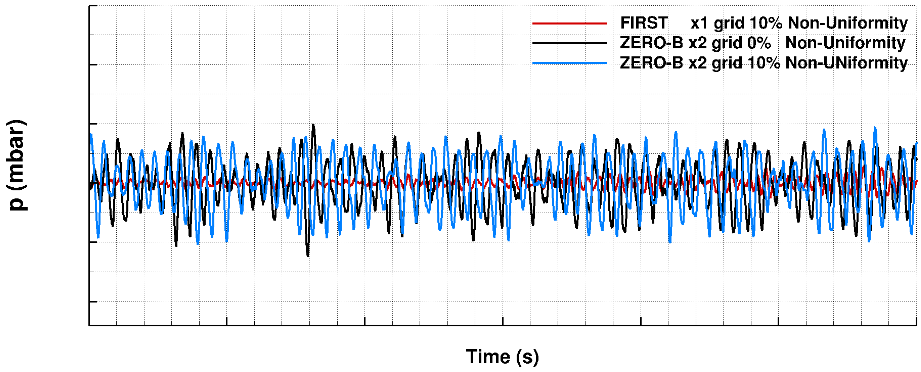

Figure 19: Non Uniform Combustion Effect on Unsteady Pressure over Time

DOI: 10.13009/EUCASS2017-430

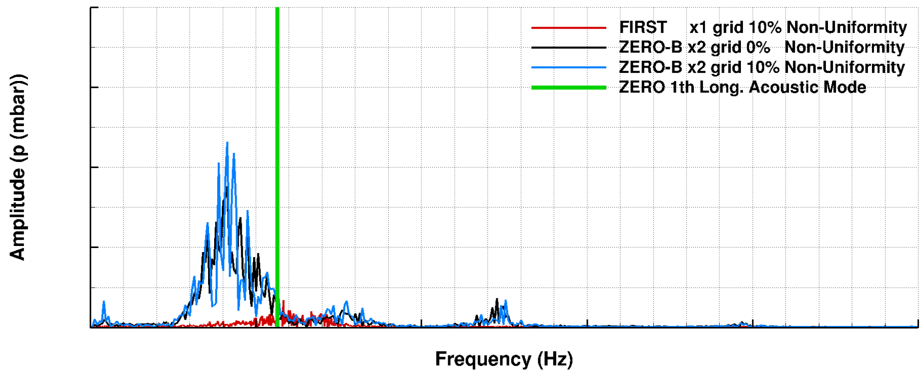

Figure 20: Non Uniform Combustion Effect on Unsteady Pressure Spectra

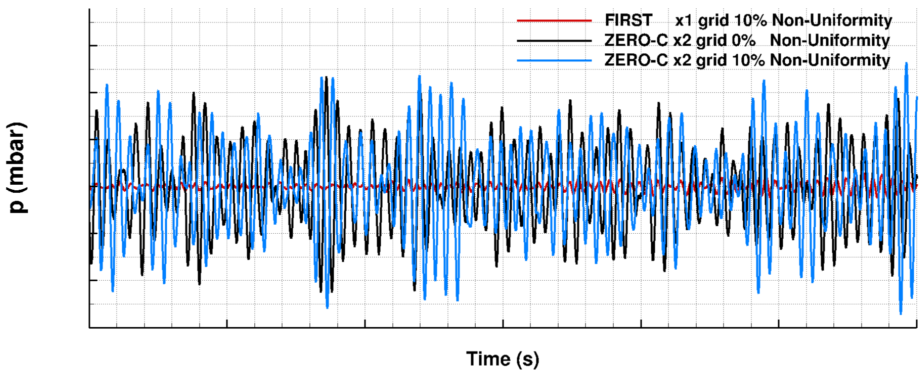

Figure 21: Non Uniform Combustion Effect on Unsteady Pressure over Time

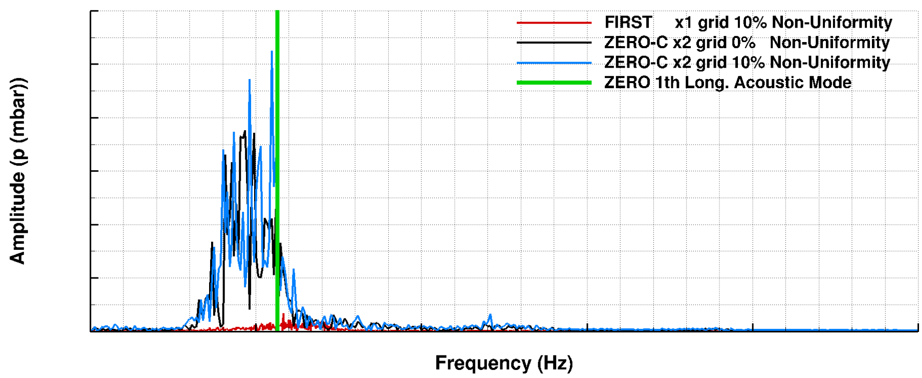

Figure 22: Non Uniform Combustion Effect on Pressure Spectra

The comparison between simplified SRM aft-finocyl geometries is presented in Fig23 and 24. ZERO-A and ZERO-B geometries are very similar, the only difference lays in the shape of the connection region, steep in the former and gradual in the latter, whereas in ZERO-C, the connection region is totally absent. Results computed for ZERO-A and ZERO-B are essentially undistinguishable in terms of both amplitudes and frequencies of pressure oscillations. When the connection region is removed, as the ZERO-C case, the scenario is completely different: the internal flowfield changes because shear layer detachment point moves downstream placing itself around the corner of the aft-finocyl region. Respect to ZERO-A/B the amplitude of pressure oscillations is 70% higher and vorticity frequency is extremely close to the first longitudinal acoustic mode of the chamber enhancing the feedback-loop.

DOI: 10.13009/EUCASS2017-430

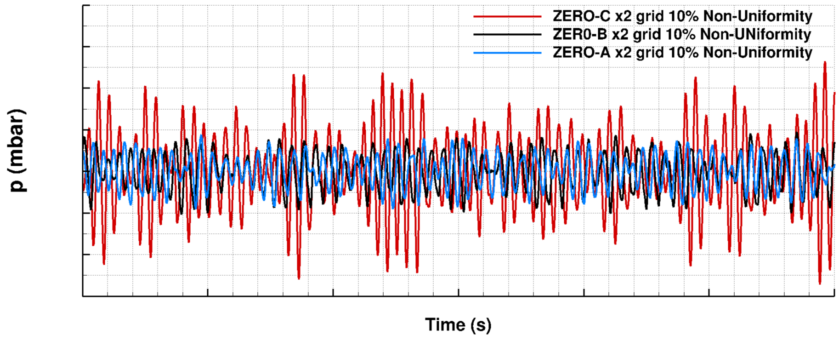

Figure 23: Non Uniform Combustion Effect on Unsteady Pressure over Time

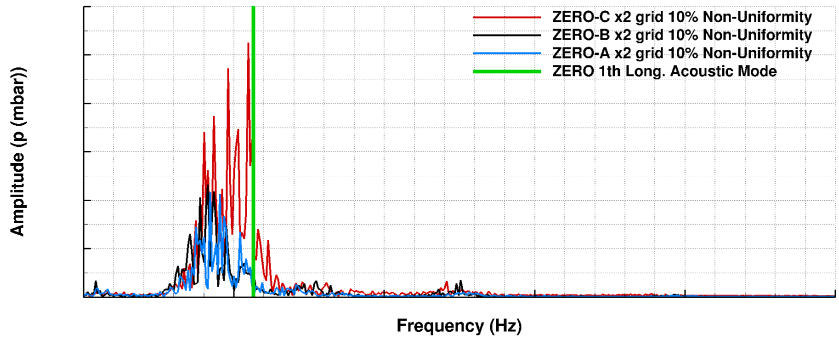

Figure 24: Non Uniform Combustion Effect on Pressure Spectra

5. Conclusions

Numerical simulations based on ILES approach and simplified non uniform combustion model for aft-finocyl SRM has been presented. Amplitudes and frequencies of pressure oscillations are strongly affected by accuracy order, mesh resolution and sub-grid models. Since the purpose is to characterise pressure oscillations in limit cycle condition, in terms of both amplitude and frequencies, a statistically steady solution is computed and discussed for simplified aft-finocyl geometries of a possible booster or first stage. The geometrical configuration is related to an early phase of the firing when head-end pressure assumes its maximum value and the aft-part/finocyl region is at around the maximum propellant burning surface condition. Several sub-grid models of the ILES approach are developed and tested in the frame of 2^{nd} order TVD schemes. Pressure oscillations features are dramatically affected by the shape of slope limiters. A trade-off between robustness of numerical method and minimization of artificial dissipation effects arises and a new limiter, named MS, has been proposed and applied. Very high levels of pressure oscillations amplitude are observed in FIRST SRM geometry. The introduction of a simplified non uniform combustion model reduces the amplitude of pressure oscillations. The more the non uniformity percentage value is high the more amplitude decreases, up to nullify itself for values greater then 10%. Three different after-finocyl geometries, ZERO-A/B/C, have been simulated, they are characterised by the same volume of the star region but different shapes of the intermediate region between cylinder and aft-star. The role of geometry on development of peculiar vorticity patterns which may be coupled with chamber acoustic modes in a feedback-loop, leading to pressure oscillations onset, is investigated. Since the shear layer detachment point is located at the end of the cylindrical part, the port area shape in the aft-finocyl region affects the coupling between vorticity field and acoustics. However ZERO-A and ZERO-B geometries exhibit the same amplitude level of pressure oscillations. The unique cavity of ZERO-C case enhances the feed-back loop and, as a consequence, pressure oscillations amplitude raises up. Convergence analysis shows pressure oscillations phenomenon is strongly mesh-level sensitive. In the present simulations, any interactions between vorticity generation and dynamics and non uniform combustion model do not showed up.

DOI: 10.13009/EUCASS2017-430

Acknowledgements

This work is supported and funded by the ESA-ESRIN/Contract No. 4000101871/10/I/JD. All the required motor data of VEGA SRMs have been kindly granted by ESA ESRIN Integrated Project Team.

VEGA launch vehicle was developed within a European Program promoted by the European Space Agency (ESA), as a cooperative project with Member States within the ESA framework. VEGA Programme was been managed by an Integrated Project Team that, under the responsibility of the European Space Agency, involved also staff from the Italian (ASI) and French (CNES) Space Agencies.

The POD-Y was developed first under CNES funding and then under ESA Contract No. 4000108839/13/F/MT with Herakles (France).

References

[1] Brown, R., Dunlap, R., Young, S., and Waugh, R., "Vortex shedding as a source of acoustic energy in segmented solid rockets," *Journal of Spacecraft and Rockets*, Vol. 18, No. 4, 1981, pp. 312–319.

[2] Blomshield, F. S. and Mathes, H., "Pressure oscillations in post-challenger space shuttle redesigned solid rocket motors," *Journal of Propulsion and Power*, Vol. 9, No. 2, 1993, pp. 217–221.

[3] Dotson, K., Koshigoe, S., and Pace, K., "Vortex shedding in a large solid rocket motor without inhibitors at the segment interfaces," *Journal of Propulsion and Power*, Vol. 13, No. 2, 1997, pp. 197–206.

[4] Scippa, S., Pascal, P., and Zanier, F., "Ariane 5-MPS - Chamber pressure oscillations full scale firing results: Analysis and further studies," *30th Joint Propulsion Conference and Exhibit*, Joint Propulsion Conferences, American Institute of Aeronautics and Astronautics, jun 1994.

[5] Mason, D., Morstadt, R., Cannon, S., Gross, E., and Nielsen, D., "Pressure oscillations and structural vibrations in Space Shuttle RSRM and ETM-3 Motors," *AIAA Paper*, Vol. 3898, 2004.

[6] Cavallini, E., Paglia, F., and Favini, B., "Analysis & Reconstruction of Pressure Oscillations during P80 Steady-State of VEGA Flights," AIAA, July 2017, 5^{rd} AIAA/ASME/SAE/ASEE Joint Propulsion Conference and Exhibit, Atlanta, Georgia.

[7] Di Mascio, A., Cavallini, E., Favini, B., and Neri, A., "Numerical Simulation of 3D Unsteady Flowfield in Aft-Finocyl Solid Rocket Motor," AIAA-2014-4015, July 2014, 50^{th} AIAA/ASME/SAE/ASEE Joint Propulsion Conference and Exhibit, AIAA Propulsion Energy Forum 2014, Cincinnati, Ohio.

[8] Di Mascio, A., Cavallini, E., Favini, B., and Neri, A., "Vortex-Sound Generation and Thrust Unsteadiness in Aft-Finocyl Solid Rocket Motor," Propulsion and Energy Forum, American Institute of Aeronautics and Astronautics, July 2015, AIAA Paper 2015-3974, AIAA Propulsion & Energy Forum 2015, Cleveland, Florida.

[9] Di Mascio, A., Cavallini, E., Favini, B., and Neri, A., "Vorticity Patterns, Sound Generation, Pressure and Thrust Oscillations in Aft-Finocyl SRM," Paper n. SP2016 3125298, May 2016, Space Propulsion 2016, Rome, Italy.

[10] Cavallini, E., Favini, B., and Neri, A., "Motor Scale and Propellant Geometry Effects on Pressure Oscillations in Aft-Finocyl Solid Rocket Motors," Propulsion and Energy Forum, American Institute of Aeronautics and Astronautics, July 2016, AIAA Paper 2016-4793, AIAA Propulsion Energy Forum 2016, Salt Lake City, UT.

[11] Cavallini, E., Favini, B., and Neri, A., "Q1D Modelling of Vortex-Driven Pressure Oscillations in Aft-Finocyl SRMs with Submerged Nozzle Cavity," Propulsion and Energy Forum, American Institute of Aeronautics and Astronautics, July 2015, AIAA Paper 2015-3975, AIAA Propulsion & Energy Forum 2015, Cleveland, Florida.

[12] Cavallini, E., Favini, B., and Neri, A., "Analysis of Pressure Oscillations during Ignition Transient and Steady-State of an Overloaded VEGA First Stage," AIAA-2014-4020, July 2014, 50^{th} AIAA/ASME/SAE/ASEE Joint Propulsion Conference and Exhibit, AIAA Propulsion Energy Forum 2014, Cincinnati, Ohio.

[13] Larrieu, S., Godfroy, F., Orlandi, O., Robert, E., Ciucci, A., and Cesco, N., "Demonstration of Pressure Oscillation Reduction in the Frame of New Launchers Development," EUCASS, July 2015, 6^{th} European Conference for AeroSpace Sciences, Krakov.

[14] Larrieu, S., "Demonstration of Pressure Oscillation Reduction For a New Large Monolithic Motor," 2016, Paper n. 3125096, 2-6 May, Rome, Italy.

DOI: 10.13009/EUCASS2017-430

[15] Dick, W.; Heath, M., "[American Institute of Aeronautics and Astronautics 38th AIAA/ASME/SAE/ASEE Joint Propulsion Conference & Exhibit - Indianapolis, Indiana (07 July 2002 - 10 July 2002)] 38th AIAA/ASME/SAE/ASEE Joint Propulsion Conference & Exhibit - Whole System Simulation of Solid Propellant Rockets," 2002.

[16] Scherrer, D., Chedevergne, F., Grenard, P., Troyes, J., Murrone, A., Montreuil, E., Vuillot, F., Lupoglazoff, N., Huet, M., Sainte-Rose, B., Thorigny, P., Bertier, N., Lamet, J., Le Pichon, T., Radenac, E., Nicole, A., Matuszewski, L., and Errera, M., "Recent CEDRE Applications," *AerospaceLab*, , No. 2, March 2011, pp. p. 1–28.

[17] Fabignon, Y., Anthoine, J., Davidenko, D., Devillers, R., Dupays, J., Gueyffier, D., Hijlkema, J., Lupoglazoff, N., Lamet, J., Tessé, L., Guy, A., and Erades, C., "Recent Advances in Research on Solid Rocket Propulsion," *AerospaceLab*, , No. 11, July 2016, pp. 15 pages.

[18] Roe, P. L., "Characteristic-based schemes for the Euler equations," *Annual Review of Fluid Mechanics*, Vol. 18, 1986, pp. 337–365.

[19] van Leer, B., "Towards the Ultimate Conservation Difference Scheme. II. Monotonicity and Conservation Combined in a Second-Order Scheme," *Journal of Computational Physics*, Vol. 14, March 1974, pp. 361–370.

[20] van Leer, B., "Towards the ultimate conservative difference scheme. III - Upstream-centered finite-difference schemes for ideal compressible flow. IV - A new approach to numerical convection," *Journal of Computational Physics*, Vol. 23, March 1977, pp. 263–299.